Article

Throwing in a Monkey Wrench to Test and Determine Geared Motion in the Dynamics of a Crystalline 1D-Columnar Rotor Array

Salvador Perez-Estrada, Braulio Rodríguez-Molina, Emily
F. Maverick, Saeed I. Khan, and Miguel A. Garcia-Garibay

Just Accepted

Throwing in a Monkey Wrench to Test and Determine GearedMotion in the Dynamics of a Crystalline 1D-Columnar Rotor Array

Salvador Pérez-Estrada,[1,2] Braulio Rodriguez-Molina,[1,3] Emily F. Maverick,[1] Saeed I. Khan,[1] Miguel A. Garcia-Garibay[1]*

[1]Department of Chemistry and Biochemistry, University of California, Los Angeles, California 90095-1569, United States; [2]Área Académica de Química, Centro de Investigaciones Químicas, Universidad Autónoma del Estado de Hidalgo, Ciudad del Conocimiento, Hidalgo 42184, México; [3]Instituto de Química, Universidad Nacional Autónoma de México, Circuito Exterior, Ciudad Universitaria, México, 04510, D.F., México

ABSTRACT: Crystals of molecular rotor **1** with a central 1,4-phenylene rotator linked to two molecules of the steroid mestranol were prepared with 1%, 5%, 20% and up to 40% of the analogous **2**, which contains a larger 2,3-difluorophenylene rotator and effectively acts as a monkey wrench that affects the rotation of the host. The packing motif of the desired $P3_2$ crystal form consists of 1D columns of nested rotors arranged in helical arrays with the central aromatic rotators disordered over two sites related by 85° rotation about their 1,4-axes. Rotational dynamics measured by quadrupolar echo ^{2}H NMR line shape analysis were analyzed in terms of a process model that involves degenerate 180° jumps in the fast exchange regime combined with a highly correlated and entropically demanding jump of 85° between the two dynamically disordered sites. While the enthalpic and entropic barriers for the 180° jump estimated from ^{2}H T_1 measurements were $\Delta H^{\ddagger} = 2.7 \pm 0.1$ kcal mol^{-1} and $\Delta S^{\ddagger} = -5.0 \pm 0.5$ cal mol^{-1} K^{-1}, respectively, the corresponding parameters for the slower 85° jumps, determined by line shape analysis, were $\Delta H^{\ddagger} = 2.6$ kcal mol^{-1} and $\Delta S^{\ddagger} = -23$ cal mol^{-1} K^{-1}. Increasing amounts of the larger molecular rotor **2** in the solid solution results in significant dynamic perturbations as the guest, acting as a monkey wrench, reaches values of one out of every five molecular rotors in the chain.

INTRODUCTION

The last few years have witnessed an increased interest in the field of amphidynamic crystals,[1] and their applications for the development of smart materials, crystalline molecular rotors, and molecular machines.[2,3,4] In a previous communication we reported the dynamics of molecular rotor **1** consisting of a 1,4-phenylene rotator linked to two mestranol molecules that play the role of the stator (Figure 1a, R=H).[5] Molecular rotor **1** can be crystallized in the trigonal chiral space group $P3_2$ with a packing structure that features a helical columnar array of nested molecular rotors as shown in Figures 1b and 1c, which respectively illustrate views with the 3-fold axis on the plane of the paper, and down the direction of the channel. Rather than having close face-to-face aromatic contacts, the phenylene rotators have a center-to-center distance of ca. 4.9Å. This generates sufficient space for them to have some rotational freedom and adopt two equilibrium sites related by a rotational displacement of 85° with 45:55 occupancies (Figure 1d).[5] One of the most interesting features of the one dimension)al (1D channel structure is the fact that the rotational energy potential is not determined uniquely by steric and/or electronic interactions from a relatively static structure, but rather by the variable position of the neighboring rotators. *This implies that rotational motion in these crystals requires some degree of rotator-rotator correlations.* In fact, variable
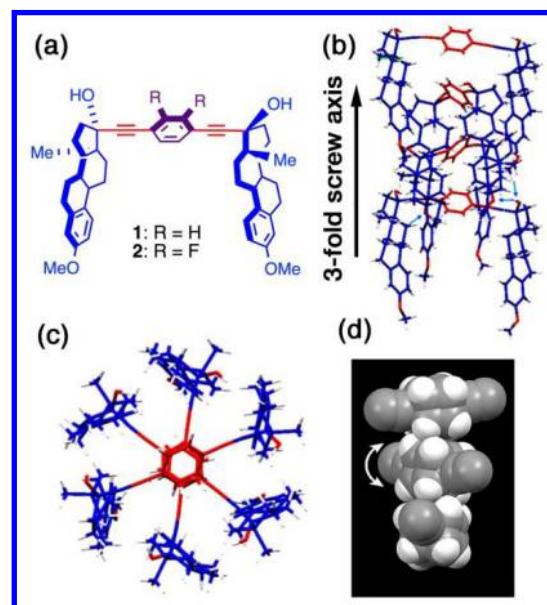

Figure 1. (a) Line structure of mestranol molecular rotors with phenylene **1** (R=H) and difluorophenylene **2** (R=F) rotators. Side (b) and top (c) views of the 1D columnar array of molecular rotors. (d) Space-filling model of phenylene rotators in the 1D chain illustrating the rotational disorder in the channel.

temperature ^{2}H NMR quadrupolar echo[6] experiments with phenylene-d_4 labeled samples revealed relatively narrow spectra (Figure 2).They could be simulated only with a somewhat counterintuitive process involving two anisochronous, or kinetically distinguishable trajectories.

The observed spectrum is different from those of most crystalline phenylene rotators, which range between theones shown in the top of Figure 2. The broad spectrum inFigure 2acorresponds to the Pake, or powder pattern, determined by the full extent of the quadrupolar coupling interaction, and is characteristic of samples where the phenylene groupsare either static, orundergoing rotation in the slow exchange regime, i.e., $k_{rot} \leq 10^4$ s^{-1}($\leq$10 kHz). The spectrum in Figure 2bcorresponds to samples where the phenylene rotator undergoes180^o flips in thefast exchange limit,which corresponds to rotational frequencies thatare ca.$\geq$10^7 s^{-1} ($\geq$10 MHz).[6,7]By contrast, the ambient temperature spectrum recorded with samples of **1** can be simulatedby a model that includes 180^o rotations in the fast exchange limit ($k_{fast} \geq$ 10 MHz) combined with slower 85°rotationsat a rate of$k_{slow} \approx$ 1.5 MHz (Figures 2c and 2d).[5]It should be noted that this motion can take values of +85° or -95° depending on the direction of measurement, however, we will simply refer to it as an 85° rotation. The trajectories suggested by the spectral simulations are consistentwith therotational C$_2$ symmetry of the phenylene group, which accounts for the 180° jumps, and the85^o relation that exists between the two disordered sites in crystal structure of **1** (Figures 1d and 3a). A schematic representation of the proposed anisochronous trajectoriescan be visualized with the help of Figure 3, the crystallographically distinct sites related by 85^o(A and B) are shown at the top (Figure 3a) and the relation that exists between the fast and slowmotion represented in Figure 3b. Considering the relativerotational frequencies, the ambient temperature spectrumrequiresthe dynamic averaging of the quadrupolar coupling interaction caused by seven or more 180° rotationsfor every 85° jump between the A and B.
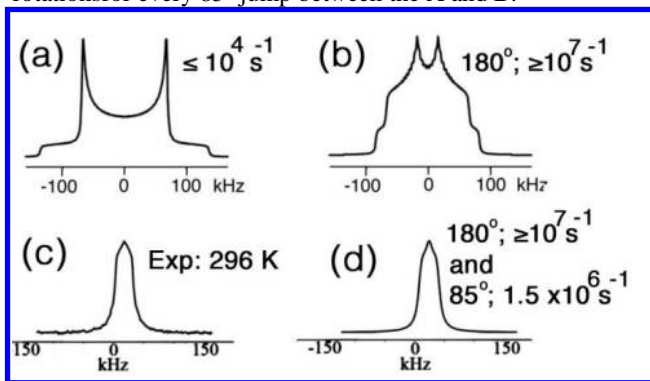

Figure 2. Representative quadrupolar echo spectra of thephenylene-d_4 rotator in the (a) slow and (b) fast exchange regimes, and (c) the experimental and (d) simulated spectra of molecular rotor **1** described in terms of fast 180° rotations and slow 85° jumps.

Further insightwas available from variable temperature ^{2}H NMR measurements, which revealed that the 85° rotation occurs with a relatively "unfavorable"activation entropy of -23 cal mol^{-1} K^{-1}, indicatingthatswitching between coordinates A and B should be slow because the need for the correlated or-concerted motion of several rotators.In this paper, searching for further insight into the proposed anisochronous and correlated model, we have explored the effects a 2,3-difluorophenylene rotator **2** (Figure 1a, R=F) added as a subs-

titutional guest to crystals of **1**.[8] We reasoned that a 2,3-difluorophenylene rotator would result in a small perturbation to the crystal lattice of **1** because the fluorine atom van der Waals radius of 1.47 Å is close to that of the hydrogen atom of *ca*. 1.20 Å.[9] Similarly, the C-F bond distance of ca. 1.34 Åis re relatively close to the C-H bond length of ca. 1.09 Å.[9]One should expect that a correlated rotational mechanism would be subject to perturbations by the slightly larger guest, which can be viewed as a *monkey wrench*.[10]It may be expected that such perturbation will beproportional to the number of rotors involved in acooperative dynamic process. That is to say, if there are$n$-rotors involved in a correlated process, the effect of added**2** would be significant when it approaches values of 1/n (assuming a random distribution). An additional element of interest in this study comes from the fact that the dipolar 2,3-difluorophenylene rotator ($\mu \approx$ 3 Debye)[11] may provide us with an alternative entry to materials with switchable macroscopic polarization.[12]Indeed, it can beshown that strongly interacting dipole chains can spontaneously adopta ferroelectric alignement,[4f] whichin cases like thiswould be able toadopteither directionalong the channel.
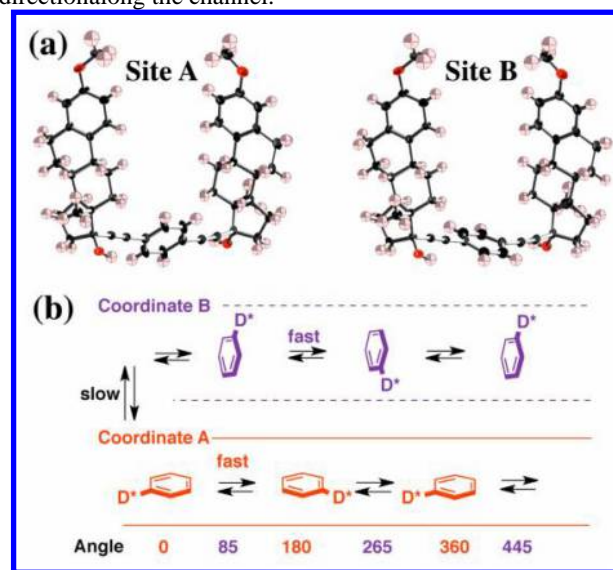

Figure 3. (a) Crystallographic sites A and B related by an angle of 85° and (b) the dynamicsof molecular rotor **1** described in terms of fast 180° rotations that retain the identity of sites A and B, combined with a much slower exchange between those two sites (adapted from reference 3).

RESULTS AND DISCUSSION

Preparation and Characterization of Solid Solutions. Solid solutions are single phase, crystalline materials that retain the crystal structure of the host with varying amounts of guest.[13] Solid solutions where the guest occupies lattice positions in a random manner are known as substitutional solid solutions.[8,13b] Solid solutions, or mixed crystals,have played an important role in the development of solid state photochemistry,[14] photophysics[15] and some areas of materials science.[13,16]Kitaigorodski suggested that substitutional solid solutions in molecular crystals mayoccur between components that have a coefficient of structural similarity that is greater than 85%.[8]With a difference of only 2 small atoms in a relatively large structure, and based on their molecular volumes, one can estimate a coefficient ofstructural similarity between **1** and **2** of ca. 98.6%, which makes them excellent candidates.

To test that, samples of molecular rotors **1** and **2** and their phenylene deuterated isotopologues were obtained by Sonogashira coupling of commercial mestranol with the corresponding 1,4-dibromo-phenylene[5] and 2,3-difluoro-1,4-trifluoromethansulfonylbenzene, respectively. We targeted solid solutions in the columnar $P3_2$ lattice of molecular rotor**1** with increasing amounts of **2**, *i.e.*,**1**:**2** = 99:1, 95:5, 80:20 and 60:40.Solid solutions $\mathbf{1}_{(1-x)}\mathbf{2}_x$ with x=0.01 and 0.05 were reliably prepared by slow evaporation at room temperature from 4:1 dichlomethane-acetonitrile solutions. In the case of x=0.2 and 0.4, solid solutions were also obtained by solvent (acetone) assisted mechanochemical crystallization.[17] We observed thatthe slow evaporation method at ratios past 20% of molecular rotor **2**resulted in phase segregation with concomitant crystallization ofthe alternative $P2_12_12_1$polymorph.[18]The formation of the$P3_2$ phase could beconfirmed by powder X-ray diffraction (PXRD), infrared spectroscopy (IR) and
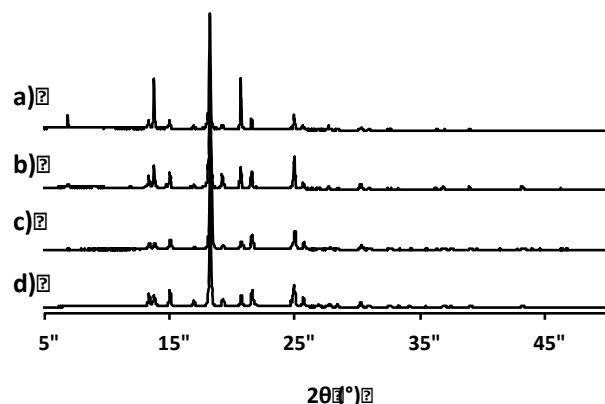

Figure 4. Powder X-ray diffraction patterns of the $P3_2$ crystal lattice of solid solutions $\mathbf{1}_{(1-x)}\mathbf{2}_x$ with a) x=0.01, b) x=0.05, c) x=0.2 and d) pure molecular rotor **1**.

differential scanning calorimetry (DSC). Diffraction patterns of solid solutions $\mathbf{1}_{(1-x)}\mathbf{2}_x$x=0.01, 0.05, 0.2 and 0.4 showed full agreement with that of molecular rotor **1** in the $P3_2$ form (Figure 4 and Figure S19). Attenuated total reflectance Fourier transform infrared spectroscopy (ATR-FTIR) can help distinguish between the $P3_2$ and $P2_12_12_1$polymorphs which have distinct fingerprint patterns, includinga characteristic OH stretch band near 3530 cm^{-1} for the$P3_2$ polymorph (Figures S7, S8,and S9 SI section). As the DSC analysis of the solid solutions $\mathbf{1}_{(1-x)}\mathbf{2}_x$ x=0.01, 0.05 and 0.2showed single endothermic transitions (Figures S12-S18), the method was particularly useful to identify mixtures of phases. DSC analyzes of pure **1** and **2** showed endothermic transitions between 250-255 °C and 231-235 °C, respectively; whereas those of dilute solid solutions $\mathbf{1}_{(1-x)}\mathbf{2}_x$ x=0.01, 0.05 are close to the pure **1** at 247-254 °C and 246-254 °C, respectively. As expected, the solid solution$\mathbf{1}_{(1-x)}\mathbf{2}_x$ x=0.2 displayed an endothermic transition at a lower temperatures of 231-239 °C. In the case of$\mathbf{1}_{(1-x)}\mathbf{2}_x$ x=0.4 two close endothermic transition peaks were observed at 225 °C and 235 °C, suggesting that the sample crystallizes with some degree of heterogeneity

We were able to grow single crystals of the solid solution $\mathbf{1}_{(1-x)}\mathbf{2}_x$, x=0.2 and, as expected, the structure solution at 100 K was obtained in the same space group as pure **1**, $P3_2$ (Table 1 and Figure S20). Similarly, the phenylene rotator is disordered over two positions with occupancies of 44:56 related by an angle of 83.1°. As expected for the 20% mol content of the

molecular rotor **2**, the refinement was consistent with a fluorine content of 0.4.While there is uncertainty related to the low fluorine content and the quality of mixed crystal specimens, the structure solution for the electron density of the fluorine atoms at 100 K was localized in one of the four disordered sites (Figure 5). Thisindicatesthat the four crystallographically different positions are not isoenergetic.A simple computational model was built with the X-ray coordinates of a central difluorophenylene and two phenylene neighbors on each side but with the full steroid structures included. This modelshowed thatthe energetics of placing the fluorine atoms in sites 1-4 (Figure 5) have relative values of 0, 2.0, 2.8 and 3.8 kcal/mol. These values are in good qualitative agreement with the X-ray structure and with ^{2}H NMR results described below.

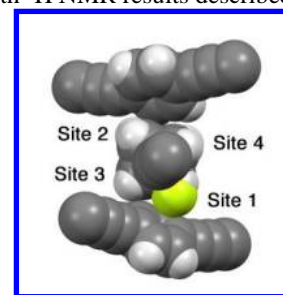**Figure 5.** View of the X-ray structure solution of the $P3_2$ mixed single crystal $\mathbf{1}_{(1-x)}\mathbf{2}_x$ x=0.2at 100K illustrating the position of the difluorophenylene rotator with respect to its two closest neighbors. The figure suggests that the *ortho*-fluorine atoms, at equilibrium, prefer one of the four possible sites (i.e., Site 1) at 100 K.

Comparing the unit cell parameters of $\mathbf{1}_{(1-x)}\mathbf{2}_x$ x=0.2 to those obtained from the pure molecular rotor **1** one can see that the axes are slightly longer in the solid solution, resulting in a larger unit cell volume (Table 1). We took advantage of single crystalline specimens to document the macroscopic homogeneity of the solid solutions. We determined that different crystals and different fragments of various single crystals have the same composition, suggesting that the host composition does not vary as the total concentration in solution changes during crystallization, and that it does not accumulate in specific sectors of the crystal structure. With well characterized samples in hand we proceeded to investigate the dynamics of the host phenylene (Ph) and guest 2,3-difluorophenylene (F_2Ph) rotators in the solid solutions $\mathbf{1}_{(1-x)}\mathbf{2}_x$.

Table 1. Unit cell parameters of the solid solution $\mathbf{1}_{(1-x)}\mathbf{2}_x$, x=0.2 and host crystal 1 in the $P3_2$space group.

	Crystal 1	Solid Solution
X-ray source	Synchrotron	Mo K_α
Wavelength (Å)	0.77490	0.71073
T (K)	100	100
a (Å)	14.7106(4)	14.758(4)
b(Å)	14.7106(4)	14.758(4)
c (Å)	14.6565(7)	14.683(4)
V (Å^3)	2746.76(17)	2769.7(12)

Activation Parameters for the 180° Rotation of Crystal Host 1 by ^{2}H NMR Spin-Lattice Relaxation. As previously noted, line shape analysis of quadrupolar echo ^{2}H NMR spectra required the 180° rotations in the $P3_2$ form of molecular rotor **1** tooccur in the fast exchange regime (k_{rot}>10^7 s^{-1}) in the

temperature range between 155 K and 296 K. Knowing that dynamic processes with rotational correlation times (τ_c in Eq. 1) in this regime approach theLarmor frequency of common magnetic nuclei($\omega_0 = 2\pi\nu_0$in Eq. 2), we decidedto take advantage of variable temperature (VT) spin-lattice relaxation T_1 measurements to determine the activation energy E_a and pre-exponential factorτ_0^{-1} (Eq. 1).[19]To accomplish that, one can substitute theτ_c in the Kubo-Tomita relaxation expression[19b] (Eq. 2) by Eq. 1.

$$\tau_c^{-1} = \tau_o^{-1} \exp(-E_a/RT) \qquad \text{(Eq. 1)}$$

$$T_1^{-1} = C[\tau_c(1 + \omega_o^2\tau_c^2)^{-1} + 4\tau_c(1 - 4\omega_o^2\tau_c^2)^{-1}] \qquad \text{(Eq. 2)}$$

To obtain information on the dynamicsof the phenylene rotator werecorded ^{2}H T_1 experiments with a ^{2}H Larmor frequency ν_0 = $\omega_0/2\pi$ = 92 MHz at 14.092 Tesla onsamples of phenylene rotator$\mathbf{1}\text{-}\boldsymbol{d_4}$. We collected$T_1$ data using a saturation recovery pulse sequence in the temperature range of 160 K to 295 K.We confirmed asingle exponential behaviorfor recovery kinetics at all temperatures measured and founda T_1 minimum at 175 K. As shown in Figure 6, the experimental T_1values as a function of the temperature were fitted to the Kubo-Tomita equation (Eq. 2), giving an activation energy of E_a=3.2$\pm$0.07kcal mol^{-1} and a pre-exponential factor τ_o^{-1}=1$\pm$0.2x10^{12} s^{-1}.As expected, these values are greater than those previously determined by ^{2}H NMR line shape analysisfor the 85° jump, which has aslightly smaller barrier ofE_a=2.6 kcal mol^{-1}anda pre-exponential factorτ_0^{-1}=1.2x10^8 s^{-1}, which is four orders of magnitude smaller.[5]

The pre-exponential factor (τ_0^{-1}) arising from ^{2}H T_1 data for the 180° rotations is consistent with an elementary process determined by the frequency of the torsional mode that must be thermally activated for the rotator to overcome the barrier, *i.e.*, τ_0^{-1} = $\nu_{torsion}$.[1,20] This is in stark contrast with the pre-exponential factor τ_0^{-1} = 10^8 s^{-1} for the 85° jumps, which reflects an entropically demanding process. It should be noted that site exchange rates calculated from the activation parameters for the 180° rotation, 4.9x10^9 s^{-1} at 296 K and 3.9x10^7 s^{-1} at 155 K, are consistent with the fast exchange frequency ($>10^7$ s^{-1}) required by the ^{2}H NMR line shape simulations.
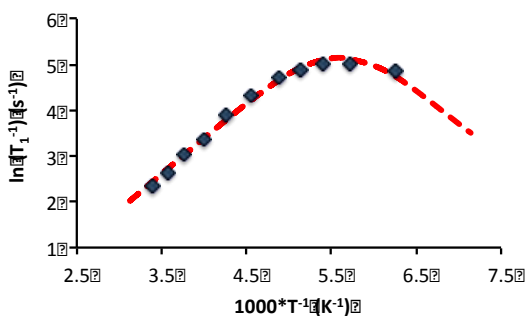

Figure 6. ^{2}H NMR Spin-lattice relaxation (T_1) experiments with molecular rotor $\mathbf{1}$recorded at 92 MHz from 160-295 K. The solid diamonds are the experimental data points and the red dotted line is the Kubo-Tomita fit to the experimental data.

Rotational Dynamics by Quadrupolar Echo ^{2}H NMR Line Shape Analysis of Solid Solutions. With dynamic information for the pure crystals of $\mathbf{1}$ and the experimental tools neededto characterized the 180° and 85° rotational dynamics, we moved on to characterize therotational motion of the host phenylene and guest difluorophenylene in solid solutions $\mathbf{1}_{(1-x)}\mathbf{2}_x$.Quadrupolar echo VT^{2}H NMR experiments were performed at 46 MHz (7.046 Tesla)with microcrystalline samples using either of the two deuterated components,$\mathbf{1}\text{-}\boldsymbol{d}_{4(1-x)}\mathbf{2}_x$ or $\mathbf{1}_{(1-x)}\mathbf{2}\text{-}\boldsymbol{d}_{2(x)}$.
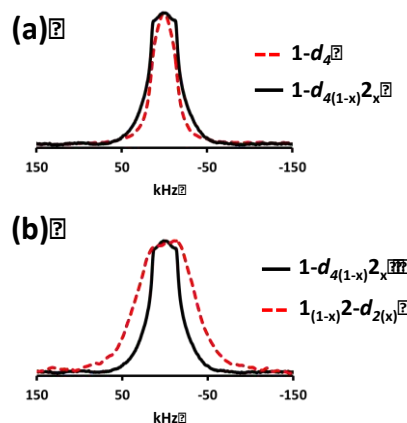
Figure 7. ^{2}H NMR spectra measured at 296 K of (a) $\mathbf{1}\text{-}\boldsymbol{d_4}$ (red dotted line) and$\mathbf{1}\text{-}\boldsymbol{d}_{4(1-x)}\mathbf{2}_x$x=0.2 (black line), and (b) $\mathbf{1}\text{-}\boldsymbol{d}_{4(1-x)}\mathbf{2}_x$ x=0.2 (blackline) and $\mathbf{1}_{(1-x)}\mathbf{2}\text{-}\boldsymbol{d}_{2(x)}$ x=0.2 (red dottedline).

Spectral changes as a function of increasing amounts of the difluorophenylene rotor $\mathbf{2}$ resulted in some broadening that depended on the amount of guest and the temperature of the experiment. Effects on the rotational motion of the phenylene host determined by measurements carried out with solid solutions $\mathbf{1}\text{-}\boldsymbol{d}_{4(1-x)}\mathbf{2}_x$ x=0.01, 0.05, 0.2 in the range of 145 K to 296 K were relatively small, as the spectra were very similar to those reported for the host crystal $\mathbf{1}\text{-}\boldsymbol{d_4}$. Particularly, the room temperature spectra of the phenylene rotator in solid solutions $\mathbf{1}\text{-}\boldsymbol{d}_{4(1-x)}\mathbf{2}_x$ x=0.01 and 0.05 are identical to that of the pure crystal host $\mathbf{1}\text{-}\boldsymbol{d_4}$(not shown).However, an increase in the amount of the difluorophenylene rotator to 20% in solid solution$\mathbf{1}\text{-}\boldsymbol{d}_{4(1-x)}\mathbf{2}_x$ x=0.2 resulted ina considerably broader spectrum with a flatter top (Figure 7a,dotted), suggestingthat rotational motion of the host rotators is affected when the guest reaches values corresponding to one host for every four guests. This initial resultindicated that perturbations at guest/hosts loading levels of 1/100 and 5/100 are not significant to alter the postulated correlated motions. However,perturbations at loading levels of 1/5 are significant, indicatingthat correlated motions involve a relatively small number of rotators in the 1D chain. Not surprisingly, when the rotational motion of the fluorinated phenylene host$\mathbf{2}\text{-}\boldsymbol{d_2}$ is analyzed at the same guest loading of 20%($\mathbf{1}_{(1-x)}\mathbf{2}\text{-}\boldsymbol{d}_{2(x)}$ x= 0.2), one can see significantly more broadening(Figure 7b, red dottedline), which is an indication that the motion of the larger hostin the same channel structureis more hindered.

Spectral changes as a function of decreasing temperature for the solid solutions were similar to those previously observed for crystals of host $\mathbf{1}$, with some broadening resultingfrom the slowing rotations as the temperature changes from 296 K to 196 K. These results are illustrated in Figure 8with two sets of spectra from measurements carried out with solid solutions containing 20% of the difluorophenylene host (i.e., $\mathbf{1}_{(1-x)}\mathbf{2}_x$

x=0.2). The spectra shown in Figure 8a correspond to samples where the host phenylene rotator is deuterated ($\mathbf{1}\text{-}d_{4(1-x)}\mathbf{2}_x$ x=0.2), and those on the right (Figure 8b) to samples wherethe NMR label is on the fluorinated guest($\mathbf{1}_{(1-x)}\mathbf{2}\text{-}d_{2x}$ x=0.2). One can see that the spectra of the two solid solutions gradually became broader at the lower temperatures as previously reported for crystals of$\mathbf{1}\text{-}d_4$.
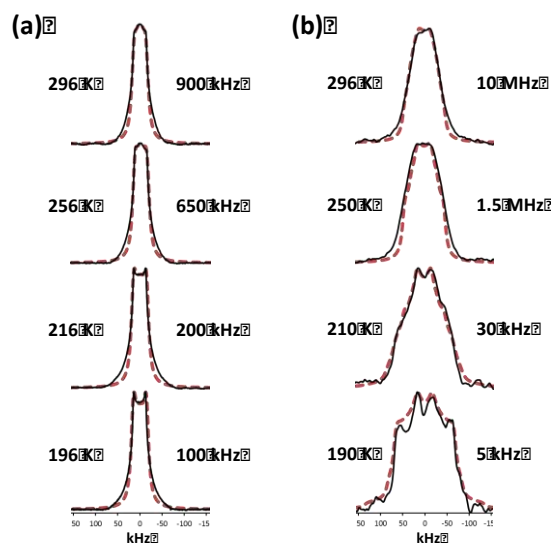

(a) **(b)**

Figure 8. ^{2}H NMR spectra recorded at 46 MHz of solid solutions (a) $\mathbf{1}\text{-}d_{4(1-x)}\mathbf{2}_x$ x=0.2 and (b) $\mathbf{1}_{(1-x)}\mathbf{2}\text{-}d_{2(x)}$ x=0.2. The black solid lines correspond to the experimental spectra and the red dotted lines to the simulation. The frequency shown in thesimulated spectra corresponds to the 85° switch, as the 180° jumpsremain in the fast exchange limit,above 10 MHz.

Line shape analysis of the spectra obtained from the phenylene rotator in the solid solution$\mathbf{1}\text{-}d_{4(1-x)}\mathbf{2}_x$ x=0.2 with the model previously used for the host crystal gave good results with a fast 180° rotation and a slow 85°site exchange.The frequencies of the latter varied from 100 kHz at 196 K to 900 kHz at 296 K, as indicated in Figure 8a. By contrast, spectral simulation for the fluorophenylene rotator in samples of $\mathbf{1}_{(1-x)}\mathbf{2}\text{-}d_{2(x)}$ x=0.2 shown in Figure 8b turned out to be more complicated. Failed attempts to reproduce the broader experimental spectra with the same mechanism included trajectories where either or both ofthe 180° and 85° jumps were considerably slower. After that, we varied the magnitude of the short jump angle and explored distributions of frequencies that might arise from structural heterogeneities in the sample.Neither set of simulations resulted in a spectrum that could match the experiment.Eventually, recognizingthat the occupation of the fluorine atoms in the crystal structure is notequally distributed over all four previously degenerate sites, we found that a three-site model involving180° rotation in the fast exchange regime, combined with slow 85° (or -95°)jumpsreproduced the experimental spectrawhen the slow process variedbetween 5 kHz and 10 MHz (Figure 8b). It appears that the broadening in this case results from the sampling of orientations rather than from slowing the dynamics of the original four sites. The proposed difference between the trajectories responsible for the spectra shown in Figure 8a and 8b is indicated in Scheme 1a and 1b, respectively. The key distinction between the two models is that the difluorophenylene rotator is unable to occupy one of the sites that is otherwise available to the phenylene rotator.

Having established viable dynamic models for the motion of the two components we collected data from the other solid solutions. Variable temperature ^{2}H NMR spectral data from the phenylene rotator were obtained with samples $\mathbf{1}\text{-}d_{4(1-x)}\mathbf{2}_x$ x=0.01, 0.05 and 0.2 and the Arrhenius and Eyring plots for the dynamics of the slower 85° rotation gave results that are similar to those observed in crystal host $\mathbf{1}$.[5]The corresponding

Scheme 1
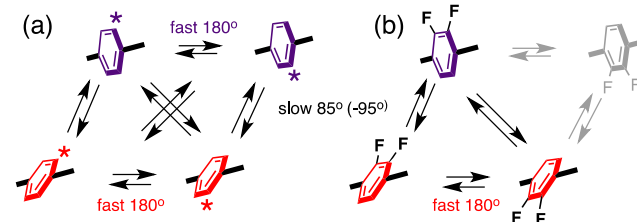
values, summarized in Table 2 in entries 3-5, showed a slight increase in the activation enthalpies and activation entropies, which take values that range from 1.6 to 2.4 kcal mol^{-1} and -19.2 to -23 cal mol^{-1}K^{-1}, respectively. It is interesting to note that the lowest concentrations of the difluorophenylene guest, 1% and 5%, actually made the rotation of the host slightly easier with slightly smaller activation enthalpies and activation entropies that are slightly less negative, which also supportsthesuggestionthat the 85° rotation occurs as a collective event, rather than in an isolated manner.

The spectra from solid solutions $\mathbf{1}_{(1-x)}\mathbf{2}\text{-}d_{2(x)}$ x=0.05, 0.2 did not show significant changes between 296 K and 250 K, but broadened significantly in going from 230 K to 190 K. We did not perform quadrupolar echo ^{2}H NMR experiments with samples of$\mathbf{1}_{(1-x)}\mathbf{2}\text{-}d_{2(x)}$ x=0.01 because of the low concentration of deuterium in the sample. Interestingly, the Arrhenius plot for the slow 85° difluorophenylene rotator jump in $\mathbf{1}_{(1-x)}\mathbf{2}\text{-}d_{2(x)}$ x=0.05 and $\mathbf{1}_{(1-x)}\mathbf{2}\text{-}d_{2(x)}$ x=0.2 revealed activation energies of E_a=6.6±0.5 and8.4±0.5 kcal mol^{-1} and pre-exponential factors of τ_0^{-1}=7.5x10^{11}±3 and 2.3x10^{13}±3 s^{-1}(Table 2, entries 6 and 7)which are considerably greater than those of the host phenylene in $\mathbf{1}\text{-}d_{4(1-x)}\mathbf{2}_x$ x=0.05 and 0.2. The corresponding enthalpies of activation for $\mathbf{1}_{(1-x)}\mathbf{2}\text{-}d_{2(x)}$ x=0.05 and $\mathbf{1}_{(1-x)}\mathbf{2}\text{-}d_{2(x)}$ x=0.2are $\Delta H^{\neq}$=6.0±0.5 and 8.0±0.5 kcal mol^{-1}, and entropies of activation change to more positive values, $\Delta S^{\neq}$=-6.0±2.1 and 1.0±2.2 cal mol^{-1} K^{-1}, suggesting that rotation of the difluorophenylene group is more of an isolated event, unable to participate in a correlated process that involves the collective motion of several rotators. It is worth noting that the large pre-exponentials for the 85° rotation in the case of $\mathbf{1}_{(1-x)}\mathbf{2}\text{-}d_{2(x)}$ x=0.05 and 0.2 result in a relatively high ambient temperature frequency despite its significantly higher energy barrier. However, with a high temperature coefficient, its rotational motion decelerates rapidly as the temperature goes down.

Rotational Dynamics of $\mathbf{2}\text{-}d_2$ in Solid Solutions at Higher Temperatures – TheLoss of Dynamic Order. When the samples $\mathbf{1}_{(1-x)}\mathbf{2}\text{-}d_{2(x)}$ x=0.05 and 0.2 were heated in the range of 315 K to 395 K, we observed that the spectra gradually narrowed, with a peak that emerges in the middle at ca. 375 K (Figure 9). We found that the model used to simulate the lower temperature spectra was no longer adequate. A solution was found with a model that considers two different popula-

Table 2. Activation parameters for the dynamics of the host phenylene and guest difluorophenylene rotators in the 1D column array of 1 and $1_{(1-x)}2_x$ x=0.01, 0.05, 0.2.[a]

Sample	Jump Angle[b]	E_a[c]	τ_0^{-1} (s^{-1})	$\Delta H^{\neq}$[c]	$\Delta S^{\neq}$[d]
1-d_4	180	$3.2_{\pm}0.1$[e]	$1_{\pm}0.2$x 10^{12}[e]	$2.7_{\pm}0.1$[e]	$-5.0_{\pm}0.5$[e]
1-d_4	85	2.6[f]	1.2x10^8[f]	2.2[f]	-23.0[f]
1-$d_{4(1-x)}2_x$ x=0.01	85	$2.0_{\pm}0.1$	7.5x$10^8 \pm 1$	1.6 ± 0.1	-19.0 ± 0.5
1-$d_{4(1-x)}2_x$ x=0.05	85	2.2 ± 0.1	7.5x$10^8 \pm 2$	1.8 ± 0.1	-19.0 ± 0.8
1-$d_{4(1-x)}2_x$ x=0.2	85	2.9 ± 0.2	1.5x$10^8 \pm 1$	2.4 ± 0.2	-23.0 ± 0.9
$1_{(1-x)}2$-$d_{2(x)}$ x=0.05	85	6.6 ± 0.5	7.5x$10^{11} \pm 3$	6.0 ± 0.5	-6.0 ± 2.1
$1_{(1-x)}2$-$d_{2(x)}$ x=0.2	85	8.4 ± 0.5	2.3x$10^{13} \pm 3$	8.0 ± 0.5	1.0 ± 2.2

[a]Unless indicated, data was determined by quadrupolar ^{2}H NMR lineshape analysis. [b]Units are degrees (°) ; [c]kcal mol^{-1}; [d]cal mol^{-1}K^{-1}; [e]Determined by ^{2}H NMR spin-lattice relaxation; [f]Reported in ref. 5.

tions with different dynamic characteristics and fractions that vary systematicallyas a function of temperature. One population is engaged in the original three site exchange model of Scheme 1b, with fast 180° rotations and one site related by 85° andjumps occurring at ca. 30 MHz (Figure 9). The second population requires a trajectory that includes site exchange in the low MHz regime between all four sites related by 85° (and -95°) jumps. The weight of the four-site population increases with increasing temperature from 15% at 335K to 78% at 395 K. We find this result to be significant, as it implies that the correlations responsible for the low temperature behavior begin to disappear, which is reasonable for an entropically demanding process with ΔS<0, as the -TΔS terms become increasingly unfavorable. We propose the change in dynamics from three sites to four sites indicates a transition from correlated to independent rotations.
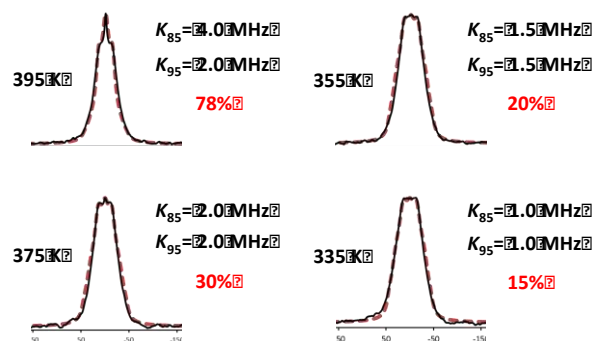
the guest:host ratio reaches the maximum value of **1**:**2** = 3:2,i.e., $1_{(1-x)}2$-$d_{2(x)}$ x=0.4. At 295K, the^{2}H NMR spectrumrecorded at 92 MHz wasrelativelybroad with a feature that projects from the center (Figure 10).The intensity of the central feature decreased as the temperature was lowered to 253 K, and then to 233 K. While reasonable spectra were obtained with simulations involving the three-site model, astatic component with a increasing contribution was required as the temperature was lowered.As shown in Figure 10,the dynamics of the three site component were consistent with those observed at lower (20%) loading, involving fast (≥10 MHz) 180° rotations and slow 85° (30 KHz - 10 MHz) jumps (Figure 10). This result suggest that jamming the channel does not have the same effect as increasingtemperatures, supporting the suggestion that correlated motion is an entropically determined process and as such is primarily affected by increasing thermal energies (TΔS).
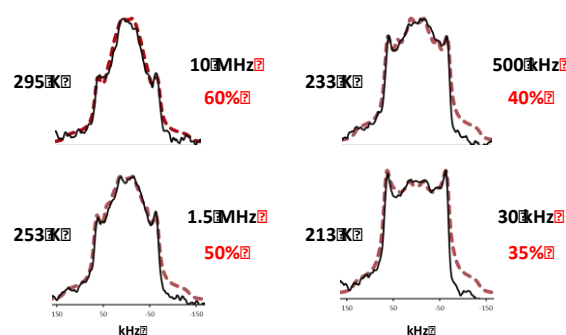

Figure 9. High temperature deuterium wideline spectra of the solid solution $1_{(1-x)}2$-$d_{2(x)}$ x=0.2 recorded at 46 MHz that showthe experimental spectra (black solid lines) and the simulated spectra (red dotted lines) obtained by considering a three sites process with fast 180° and slow 85° jumps (not shown) and a four sites process with consecutive 85° and 95° jumps. The percentage shown corresponds to the contribution of the four sites process.

To further testthe emerging model, and to determine whether the observed loss of order occurs primarily as a function of temperature, or whether it can occur as a function of increasing guest loading, we turned our attention to samples where

Figure 10. Experimental (black solid line) and simulated (red dotted line) deuterium wideline spectra of solid solution $1_{(1-x)}2$-$d_{2(x)}$ x=0.4 recorded at 92 MHz. The simulated spectra were produced considering two components of a three sites process, a static at 10 kHz (not shown) and mobile component with fast 180° jumps (≥100 MHz) and slow 85° jumps (30 KHz - 10 MHz). The frequency displayed corresponds to the 85° jump and percentage corresponds to the contribution of the mobile component.
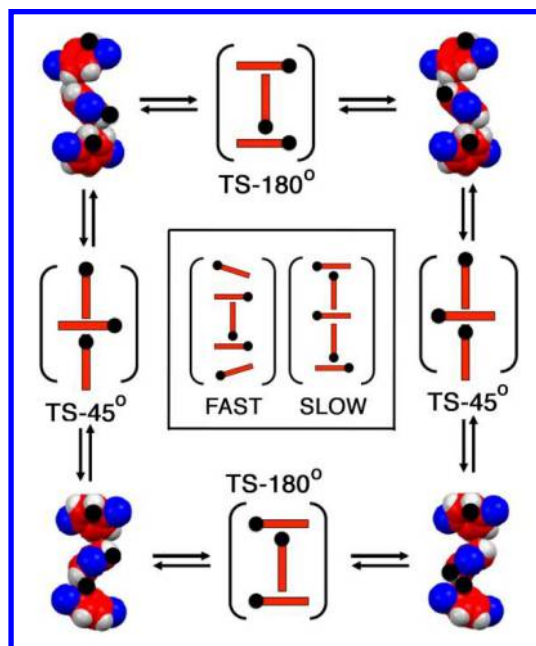
Figure 11. Mechanism for the rotation of the phenylene rotator in the 1D column of molecular rotor **1**.

A qualitative model that captures a plausible mechanism for the correlated motion is shown in Figure 11 with three rotators that have one phenylene edge labeled with a black dot. On the top and bottom horizontal we represent a process where the reference rotator at the center of the triad undergoes 180° rotation by a transition state (TS-180°) that involves relatively small displacement of the two close neighbors. By adopting orientations orthogonal to the chain direction while the central ring rotates, they would disrupt the smaller number of neighbors, making it a low entropy process. By contrast, to change the tilt of the molecules by 45° (55°) would require a transition state (TS-45°) where the two neighbors need to align along the direction of the channel, which is likely to disrupt more molecules unless two or more are engaged in the process. The effect of these two processes on the next near neighbors is represented in the center of the figure, suggesting why isolated 180° rotation would be faster than a collective motion of 45°.

CONCLUSIONS

In summary, we showed that in crystals of pure molecular rotor **1** the barrier of the 180° rotation is slightly greater, E_a=3.2±0.1 kcal mol^{-1}, than that of the 85° rotation, E_a=2.6 kcal mol^{-1}, but its pre-exponential factor is four orders of magnitude larger. The large and negative entropy of the 85° jump, $\Delta S^{\neq}$=-23 mol^{-1} K^{-1} is indicative of an entropically demanding process within the 1D column of phenylene rotators. By contrast, the entropy of the 180° jump, $\Delta S^{\neq}$=-5.0±0.5 cal mol^{-1} K^{-1}, is considerably less negative. Mixed crystals of molecular rotors **1** and **2**, **1**$_{(1-x)}$**2**-$d_{2(x)}$ x=0.01, 0.05, 0.2 and 0.4, were reliably prepared by slow solvent evaporation and solvent assisted mechanochemical crystallization. Variable temperature quadrupolar echo ^{2}H NMR experiments revealed that increasing

amounts of the guest **2** as well as lowering the temperature slows down the rotation of the host **1** and that the rotational trajectory of the host phenylene rotators is not affected by the guest 2,3-difluorophenylene rotators. Additionally, in solid solutions **1**$_{(1-x)}$**2**-$d_{2(x)}$ x=0.01 and 0.05 the 2,3-difluorophenylene rotator appears to facilitate the 85° rotation of the host phenylene rotator, as can be noted by smaller energy barriers than that of the pure molecular rotor **1**. The host phenylene rotators became slower at a ratio of 1:4 of molecular rotors **2** and **1**. On the other hand, as a result of its slightly larger size, the 85° rotation of the 2,3-difluorophenylene rotator is more encumbered and disengaged from the correlated rotation of the host phenylene rotators. This is evident from larger energy barriers and more positive entropies, E_a=6.6±0.5 to 8.6±0.5 kcal mol^{-1} and $\Delta S^{\neq}$=-6.0±2.1 to 1.0±2.2 mol^{-1} K^{-1}. However it follows the same trajectory of fast 180° and slower 85° rotation, without occupying one of the four disordered positions. This work also suggests the value of substitutional solid solutions as an additional strategy to control the properties of amphidynamic crystals and crystalline molecular machines.

ASSOCIATED CONTENT

Supporting Information

Experimental procedures, spectral data, DSC and TGA analyses, VT ^{13}C CPMAS solid state NMR, and XRPD patterns (PDF). A CIF file for single crystal X-tray analysis of solid solution solution **1**$_{(1-x)}$**2**$_x$, x=0.2 is also included. This material is available free of charge via the Internet at http://pubs.acs.org.

AUTHOR INFORMATION

Corresponding Author

* mgg@chem.ucla.edu

REFERENCES

1 (a) Vogelsberg C S.; Garcia-Garibay, M.A. Crystalline Molecular Machines: Function, Phase Order, Dimensionality, and Compotition. *Chem. Soc. Rev.*, **2012**, *41*, 1892-1910. (b) Khuong, T.-A. V.; Nuñez, J. E.; Godinez, C. E.; Garcia-Garibay, M. A. Crystalline Molecular Machines: A Quest Toward Solid-State Dynamics and Function. *Acc. Chem. Res.* **2006**, *39*, 413-422. (c) Zhang, W.; Ye, H.-Y.; Graf, R.; Spiess, H. W.; Yao, Y.F.; Zhu, R. Q.; Xiong, R.-G. Tunable and Switchable Dielectric Constant in an Amphidynamic Crystal. *J. Am. Chem. Soc.*, **2013**, *135*, 5230–5233; (d) Aguilar-Granda, A.; Pérez-Estrada, S.; Sánchez-González, E.; Álvarez, J.R.; Rodríguez-Hernández, J.; Rodríguez, M.; Roa, A. E.; Hernández-Ortega, S.; Ibarra, I. A; Rodríguez-Molina, B. Transient Porosity in Densely Packed Crystalline Carbazole–(*p*-Diethynylphenylene)–Carbazole Rotors: CO$_2$ and Acetone Sorption Properties. *J. Am. Chem. Soc.*, **2017**, *139*, 7549–7557.

2 (a) Sauvage, J.P. From Chemical Topology to Molecular Machines (Nobel Lecture). *Angew. Chem. Int. Ed.*, **2017**, 56, 11080-11093; (b) Stoddart, J.F. Mechanically Interlocked Molecules (MIMs)–Molecular Shuttles, Switches, and Machines (Nobel Lecture). *Angew. Chem. Int. Ed.*, **2017**, 56, 11094-; (c) Feringa, B. The Art of Building Small: From Molecular Switches to Motors (Nobel Lecture. *Angew. Chem. Int. Ed.*, **2017**, 56, 11060-11078.

3 Articles published on Artificial Molecular Machines Special Feature,*Proc. Natl. Acad. Sci. USA,*2018, 115.

4 Narayanan, A.; Cao, D.; Frazer, L.; Tayi, A. S.; Blackburn, A. K.; Sue, A. C.-H.; Ketterson, J. B.; Stoddart, J. F.; Stupp, S. I., Ferroelectric Polarization and Second Harmonic Generation in Supramolecular Cocrystals with Two Axes of Charge-Transfer. *J. Am. Chem. Soc.*2017, *139*, 9186—9191; (c) Erbas-Cakmak, S.; Leigh, D.A.; McTernan, C.T.; Nussbaumer, A. L. Artificial Molecular Machines. *Chem. Rev.*, **2015**, *115*, 10081–10206. (d) Abendroth, J. M.; Bushuyev, O. S.; Weiss, P.S.; Barrett, C.J. Controlling Motion at the Nanoscale: Rise of the Molecular Machines. *ACS Nano*, **2015**, *9*, 7746–7768. (e) Kottas, G. S.; Clarke, L. I.; Horinek, D.; Michl, J. Artificial Molecular Rotors, *Chem. Rev.* **2005**, *105*, 1281-1376. (f) S. W.; Solvaeson, D.; Ratner, M. A.; Michl, J.Molecular Dipole Chains: Excitations and Dissipation*,* DeLeew, *J. Phys. Chem. B*, **1998**, 102, 3876–3885.

5 Rodriguez-Molina, B.; Farfan, N.; Romero, M.; Mendez-Stivalet, J.M.; Santillan, R.; Garcia-Garibay, M.A. Anisochronous Dynamics in a Crystalline Array of Steroidal Molecular Rotors: Evidence of Correlated Motion within 1D Helical Domains. *J. Am. Chem. Soc.*, **2011**, *133*, 7280–7283.

6 (a) Spiess, H.W. Molecular Dynamics of Solid Polymers as Revealed by Deuteron NMR. *Coll. Polym. Sci.*1983, *261*, 193-209. (b) Hoatson, G.L.; Vold, R.L. ^{2}H-NMR Spectroscopy of Solids and Liquid Crystals. *NMR*Basic Princ. Prog.*1994*, *32*, 1-67. (c) Luz, Z.; Hewitt, R.C.; Meiboom, S. *J.* Deuterium Magnetic Resonance Study of a Smectic Liquid Crystal. *Chem. Phys.* **1974**, *61*, 1758-1765.

7 (a) Fyfe, C. A. Solid State NMR for Chemists. CFC Press: Guelph, Ontario, 1983. (b) Nishikiori, S. I.; Somona, T.; Iwamoto, T., In-plane and Out-of-plane Motion of Benzene Trapped in a Cd(py)2{Ag(CN)2}2 Host as Studies by Deuterium NMR. *J. Inclusion Phenom. Mol. Recognit. Chem.* **1997**, *27*, 233-243.

8 Kitaigorodski, A. I. Mixed Crystals. Springer Verlag: Berlin, 1984.

9 (a) O'Hagan, D. Understanding Organofluorine Chemistry. An Introduction to the C–F Bond.*Chem. Soc. Rev.* **2008**, *37*, 308-319. (b) Bondi, A. van der Waals Volumes and Radii. *J. Phys. Chem.*1964, *68*, 441-451. (c) Mantina, M.; Chamberlin, A. C.; Valero, R.; Cramer, C. J.; Truhlar, D. G. Consistent van der Waals Radii for the Whole Main Group. *J. Phys. Chem. A*2009, *113*, 5806-5812.

10 According to the online Merriam Webster dictionary, a monkey wrench is something that disrupts: https://www.merriam-webster.com/dictionary/monkey%20wrench (accessed Oct 17, 2018).

11 Horansky, R.D.; Clarke, L.I.; Winston, E.B.; Price, J.C.; Karlen, S.D.; Jarowski, P.D.; Santillan, R.; Garcia-Garibay, M.A. Dipolar Rotor-Rotor Interactions in a Difluorobenzene Molecular Rotor Crystal. *Phys. Rev. B*2006, 74, 054306.

12 Ostroverkhava, O. Organic Optoelectronic Materials: Mechanisms and Applications. *Chem. Rev.* **2016**, *116*, 13279-13412. (b) Jiang, X.; Zhao, S.; Lin, Z.; Luo, J.; Bristowe, P. D.; Guan, X.; Chen, C. The Role of Dipole Moment in Determining the Nonlinear Optical Behavior of Materials: *ab initio* Studies on Quaternary Molybdenum Tellurite Crystals. *J. Matter. Chem. C* 2014, *2*, 530-537.

13 (a) West, A. R. Basic Solid State Chemistry, 2nd ed.; John Wiley & Sons, Ltd: Chichester, 1999. (b) Lusi, M., Engineering Crystal Properties through Solid Solutions" *Cryst. Growth Des*. **2018**, *18*, 3704-3712. (c) Lusi, M. A Rough Guide to Molecular Solid Solutions: Design, Synthesis and Characterization of Mixed Crystals. *CrystEngComm*2018, *20*, 7042-7052.

14 (a) Ramamurthy, V.; Venkatesan, K. Photochemical Reactions of Organic Crystals. *Chem. Rev.*1987, *87*, 433-481. (b) Hochstrasser, R. M.; King, D. S. Isotopically Selective Photochemistry in Molecular Crystals. *J. Am. Chem. Soc.* **1975**, *97*, 4760-4762.

15 (a) Hochstrasser, R. M.; King, D. S.; Smith III, A. B. Spectroscopy, Photophysics, and Photochemistry of Dimethyl-s-tetrazine and Phenyl-s-tetrazine in Crystals and Mixed Crystals at Low Temperatures. *J. Am. Chem. Soc.* **1977**, *99*, 3923-3933. (b) Bolton, O.; Lee, K.; Kim, H.-J.; Lin, K. Y.; Kim. J. Activating Efficient Phosphorescence from Purely Organic Materials by Crystal Design. *Nat. Chem.* **2011**, *3*, 205-210. (c) Bolton, O.; Lee, D.; Jung, J.; Kim, J. Tuning the Photophysical Properties of Metal-Free Room Temperature Organic Phosphors via Compositional Variations in Bromobenzaldehyde/Dibromobenzene Mixed Crystals. *Chem. Matter.* **2014**, *26*, 6644-6649.

16 (a) Barth, T. F. W. Optical Properties of Mixed Crystals. *Am. J. Sci.*1930, *19*, 135-146. (b) Shao, Y.; Yang, Y. White Organic Light-Emitting Diodes Prepared by a Fused Organic Solid Solution Method. *Appl. Phys. Lett.* **2005**, *86*, 073510-073513. (c) Shao, Y.; Yang, Y. Organic Solid Solutions: Formation and Applications in Organic Light-Emitting Diodes. *Adv. Funct. Mater.* **2005**, *15*, 1781-1786. (d) Inukai, M.; Fukushima, T.; Hijikata, Y.; Ogiwara, N.; Horike, S.; Kitagawa, S. Control of Molecular Rotor Rotational Frequencies in Porous Coordination Polymers Using a Solid-Solution Approach. *J. Am. Chem. Soc.*2015, *137*, 12183-12186.

17 Friscic, T.; Childs, S. L.; Rizvi, S.A.A.; Jones, W. The Role of Solvent in Mechanochemical and Sonochemical Cocrystal Formation: A Solubility-Based Approach for Predicting Cocrystallisation Outcome. *CrystEngComm*, **2009**, *11*, 418–426.

18 Rodríguez-Molina, B.; Ochoa, M. E.; Romero, M.; Khan, S. I.; Farfán, N.; Santillán, S.; Garcia-Garibay, M. A. Conformational Polymorphism and Isomorphism of Molecular Rotors with Fluoroaromatic Rotators and Mestranol Stators. *Cryst. Growth Des.*2013, *13*, 5107-5115.

19 (a) Bakhmutov, V. I. Practical NMR Relaxation for Chemists; John Wiley & Sons Ltd, Chichester, England, 2004. (b) Kubo, R.; Tomita, K. A General Theory of Magnetic Resonance Absorption. *Phys. Soc. Jpn.* **1954**, *9*, 888-919.

20 Kawski, A. Fluorescence Anisotropy: Theory and Applications of Rotational Depolarization. *Crit. Rev. Anal. Chem.* **1993**, *23*, 459-529.

8

1
2
3
4
5
6
7
8
9
10
11
12
13
14
15
16
17
18
19
20
21
22
23
24
25
26
27
28
29
30
31
32
33
34
35
36
37
38
39
40
41
42
43
44
45
46
47
48
49
50
51
52
53
54
55
56
57
58
59
60

TOC

Geared Rotation in a Crystalline 1D-Columnar Array

9